An Introduction to Mesh Quality

M.Berzins
CPDEs Unit, School of Computer Studies, University of Leeds
Woodhouse Lane, Leeds LS2 9JT, U.K.

Abstract

The issue of mesh quality for unstructured triangular and tetrahedral meshes is considered. The theoretical background to finite element methods is used to understand the basis of present-day geometrical mesh quality indicators. Simple tetrahedral mesh quality measures using both geometrical and solution information are described. Some of the issues in mesh quality for unstructured tetrahedral meshes are illustrated by means of simple examples. These examples illustrate that the use of geometrical mesh quality measures alone may give misleading information and that mesh quality for problems modelling complex flows depends on the numerical error, the norm used to measure the error and the relationship between these quantities and the shape of the elements.

1 Introduction

The range of partial differential equations problems (p.d.e.s) solved by finite element and finite volume solvers based on triangular and tetrahedral meshes e.g. [11] [48] is rapidly increasing. The original applications problem class for many such solvers was in the area of solid mechanics and elasticity in particular. These same types of methods are now being applied to a wide range of problems in solid and fluid mechanics ranging from linear elasticity to turbulent flows. This very broad spectrum of applications naturally raises the issue of whether or not the meshes being used are appropriate for the applications being considered. The relationship between the shape of finite elements in unstructured meshes and the error that results in the numerical solution is of increasing importance as finite elements are used to solve problems with highly anisotropic and, often, very complex solutions. Strong local variations in solution component values make it difficult to assess the quality of the mesh for each component without somehow incorporating solution behaviour. In the case of mesh generation, the usual approach is to assume that the solution to the problem is such that mesh quality may be viewed as being independent of the solution [48, 32]. Indeed when no solution has been computed on the mesh this is the only way to proceed. Once a solution has been computed, the generally accepted point of view is that it is both the shape of the elements and the local solution behaviour that are important, particularly for highly directional flow problems [41, 43]. The starting point for this work is the analysis of Babuska and Aziz [10], who showed that the requirement for triangles is that there should be no large angles. This work was extended to tetrahedral elements by Krizek [27] in a similar spirit.

The intention here is not to deal with the issue of how to construct an optimal mesh but instead to consider the related issue of how the quality of an existing mesh should

be assessed given a solution. This reflects an important practical issue, particularly in three space dimensions, when a mesh generator produces a mesh of unknown quality for a complex solution. The requirement is then to assess how appropriate the mesh is for the computed solution. The ideal approach is to use a computed error estimate to assess whether or not the mesh should be refined. This error estimate should reflect not only the interpolation error caused by approximating the solution by a finite element space on a given mesh but also the discretization error of the numerical method used to approximate the p.d.e. and the choice of norm used to measure the error.

In many cases however such error estimates are not available but it is still desirable to understand whether or not the mesh is appropriate. This paper will discuss the simple mesh quality indicator of Berzins [16] based on L^2interpolation error estimates. The fundamental assumption being made is that the solution is being represented by a piecewise linear triangular or tetrahedral basis and that the function being approximated is quadratic. This assumption allows the error to be approximated by a quadratic function and the results of Nadler [36, 37] to be used for the triangular case. The resulting indicator has been shown to be related to those of Bank [12] and Weatherill [48] when geometry alone is taken into account.

The quantities used in defining the full indicator have also been used to generate [20] and modify [2] meshes in two dimensions. This paper will show that the new indicator may be used to identify which triangular or tetrahedral elements need refining and also which edge(s) should be refined. A model of boundary layer flow will be used to demonstrate how the indicator performs in identifying which triangle is best. A further simple example will show the optimum mesh will depend critically on the choice of norm used to measure the error.

The second part of the paper will consider the indicator in the case of a linear element tetrahedral mesh. A parameterised tetrahedron combined with a simple model of a solution with highly directional gradients will be used to illustrate how the new indicator identifies the effect of directionality on the linear element approximation error and how this contrasts with a purely geometrical mesh quality measure.

The conclusion of the paper is that while purely geometrical mesh quality indicators may do a good job in identifying meshing anomalies, the appropriateness of a mesh for a given solution cannot be decided using geometry alone and that although indicators based on interpolation errors may give better insight into how to stretch the mesh the only real solution is to use error estimators with an explicit geometry dependence. The material covered in these notes is taken from the surveys of Berzins [18, 19] and is partly described in its original form in [16, 17].

2 Finite Element Interpolation Error Estimates

In order to start to understand the issue of mesh quality it is necessary to review the important finite element results that form a basis for existing mesh quality measures. In order to state these results it is necessary to introduce some notation. Without loss of generality the case of linear finite elements on triangular meshes will be considered. Define the error as being the difference between the linear approximation, u_{lin} and the true solution u i.e. $e_{lin}(x,y) = u(x,y) - u_{lin}(x,y)$. The L^2 error norm over a triangle T is defined by $||e_{lin}(x,y)||_{L^2(T)}$ where

$$||e_{lin}(x,y)||^2_{L^2(T)} = \int_T (e_{lin}(x,y))^2 dxdy \ . \tag{1}$$

The H^1 error norm on a triangle T is defined by $||e_{lin}(x,y)||_{H^1(T)}$ where

$$||e_{lin}(x,y)||^2_{H^1(T)} = \int_T (e_{lin}(x,y))^2 + (\frac{\partial}{\partial x} e_{lin}(x,y))^2 + (\frac{\partial}{\partial y} e_{lin}(x,y))^2 dxdy \ . \tag{2}$$

The seminorm of the H^2 space is defined by $|u|_{2,T}$ where

$$|u|_{2,T} = \left(\sum_{|\delta|=2} \frac{2}{\delta_1 \delta_2} ||(\partial_x)^{\delta_1} (\partial_y)^{\delta_2} u||^2_{L^2(T)} \right)^{1/2} . \tag{3}$$

Aside from the notion that meshes with regular or smoothly varying element sizes are more aesthetically pleasing, the starting point for the notion of mesh quality would appear to be the analysis leading to the minimum angle condition that the smallest angle should be bounded away from zero. This perhaps originated with Zlamal [49] and is quoted by Strang and Fix [46] together with a statement regarding how *poorly shaped* triangles may have an effect on the condition number of the linear algebra problem that must be solved. This result was improved by Babuska and Aziz [10], who showed that the correct requirement for triangles was that there should be no large angles. The general results of both Zlamal and Babuska and Aziz are of the form

$$||e_{lin}(x,y)||^2_{H^1(T)} \ \leq \ \Gamma(\theta)|u|_2 \tag{4}$$

where Zlamal [49] showed that $\Gamma(\theta) = h/sin(\theta_{min})$ for the minimum angle θ_{min} of the interior angles in Figure 1. In improving this result Babuska and Aziz [10] showed that $\Gamma(\theta) = h/\Psi(\theta)$ where $\Psi(\theta)$ is a positive continuous and finite function and for $\theta \leq \gamma < \pi, \Psi(\theta) \geq \Psi(\gamma)$ where γ is a bound on the maximum interior angle of the triangle in Figure 1. Many other similar results were proved at around the same time.

More recently the monograph of Apel [9] contains a unified theory of interpolation error estimates and also describes and references these results. Apel's work also extends to tetrahedra and includes a discussion of the work of Krizek [27] and others which extends the work of Babuska and Aziz to three dimensions. Apel [4] suggests that in order to compensate for large norms of certain directional derivatives of the solution u by a small element size in this direction, it is necessary to have sharper estimates, like

$$|e_{lin}|_{1,p,T} \leq C \sum_{i=1}^{d} h_i \left| \frac{\partial u}{\partial x_i} \right|_{1,p,T} , \tag{5}$$

where d is the spatial dimension, h_i are suitably defined element sizes on the element, such as h and αh in Figure 1; P defines the type of L^P norm used and T is the element. Apel emphasises that a refined estimate on the reference element is necessary for the proof of such estimates, see [4]. Anisotropic local interpolation error estimates have been proved by Apel *et al.* for several element types (triangles, quadrilaterals, tetrahedra, triangular prisms, hexahedra, including some subparametric and non-conforming elements), for trial functions of arbitrary order, and under various smoothness assumptions on the function to be interpolated [5, 9].

Apel also stresses that anisotropic elements must be treated carefully. For example, estimate (5) is valid for simplicial elements and linear trial functions under the following

assumptions on p. In the 2D case (5) is valid for the whole range of p, $p \in [1, \infty]$. However, in the 3D case the estimate is valid for $p \in (3/2, \infty]$ for isotropic elements but only for $p \in (2, \infty]$ for anisotropic elements.

Anecdotal evidence confirms that the early theoretical results influenced mesh generation code writers. Early mesh generation papers are covered by the surveys of Shephard [44] and Thacker [47]. In these surveys there is little explicit reference to how the theoretical work has been adopted, though Thacker does say that elements should be nearly equilateral otherwise instability may result. More recent surveys by Bern and Epstein [15] and Nielson [38], do mention the theoretical results and the monographs of Carey [22] and George and Borouchaki [25] treat the subject in more detail. The perceived meshing wisdom has thus been that if possible elements should have no small or large angles. In the case of tetrahedral meshes this has has led to geometric mesh quality indicators as described in Liu and Joe [32], one example being Weatherill's edge quality estimator [48], denoted here by Q_w, for tetrahedra of volume V and edge lengths h_i:

$$Q_w = \frac{1}{8.48528V} \left[\sum_{i=1}^{6} \frac{h_i}{6} \right]^3 . \tag{6}$$

Such indicators do a good job of identifying geometric imperfections in the mesh. This is clearly an important task before any solution is computed on the mesh. The difficulty is that it is unclear that such indicators are valid for every solution on every mesh. Indeed it will be shown here that this is not the case. The ideal solution is thus to understand the relationship between the error and the mesh. The main requirement is thus for error estimators that include both solution and geometry information. Such estimators are still in their infancy, especially in 3D, but it will be shown by simple examples on tetrahedral meshes, that the accuracy in the solution can depend critically on the mesh, the numerical scheme and on any directionality present in the solution.

3 Nadler's Finite Element Error Estimator.

The decision as to whether or not (and how) a mesh should be refined should be based on an error estimate that reflects not only the interpolation error caused by approximating the solution by a finite element space on a given mesh but also the discretization error of the numerical method used to approximate the p.d.e. and the choice of norm used to measure the error. Rippa [41] makes a convincing case based on interpolation errors that long thin triangles do indeed form part of a good mesh for strongly anisotropic solutions. A good discussion of this topic also occurs in Nielson [38] and a very precise and complete mathematical analysis in Apel [9].

Berzins [16] derives a new mesh quality indicator from the work of Nadler [36] which gives a particularly appropriate expression for the interpolation error when a quadratic function is approximated by a piecewise linear function on a triangle. Consider the triangle T defined by the vertices v_1, v_2 and v_3 as shown in Figure 1 below. Let h_i be the length of the edge connecting v_i and v_{i+1} where $v_4 = v_1$.
Nadler [36] considers the case in which a quadratic function

$$u(x, y) \;=\; \frac{1}{2} \underline{x}^T \; H \; \underline{x} \text{ where } \quad \underline{x} \;=\; \begin{bmatrix} x \\ y \end{bmatrix} \tag{7}$$

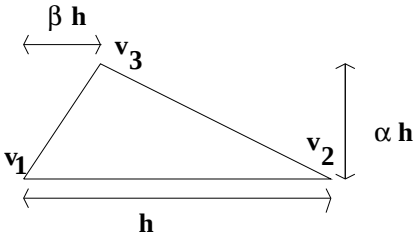

Figure 1: Babuska and Aziz example triangle.

is approximated by a linear function $u_{lin}(x, y)$, as defined by linear interpolation based on the values of u at the vertices. Denote the error by

$$e_{lin}(x, y) = u_{lin}(x, y) \ - \ u(x, y) \ . \tag{8}$$

Nadler [36], as quoted in Rippa [41], shows that

$$\int_T (e_{lin}(x, y))^2 dx \ dy \ = \ \frac{A}{180} \left[((d_1 + d_2 + d_3)^2 + {d_1}^2 + d_2^2 + d_3^3 \right] \tag{9}$$

where A is the area of the triangle and $d_i = \frac{1}{2}(v_{i+1} - v_i)^T \ H \ (v_{i+1} - v_i)$ is the scaled second derivative of the quadratic function along the edge connecting v_i and v_{i+1}.
Example 1 In the case when the matrix H is positive definite with diagonal entries p^2 and q^2 and symmetric off-diagonal entries pq then

$$d_i = (p \ \Delta x_i \ + \ q \ \Delta y_i)^2 \ \text{ where } v_{i+1} - v_i = [\Delta x_i, \Delta y_i]^T.$$

In the case of the triangle in Figure 1, assuming that x and y are in the horizontal and vertical directions respectively, the values of d_i are $d_1 = p^2 h^2$, $d_2 = h^2(-(1-\beta)p \ + \alpha q)^2$ and $d_3 = h^2(\beta p - \alpha q)^2$.
Example 2 In contrast when the solution is $u(x, y) = \frac{1}{2}(px^2 + 2qxy + py^2)$ the matrix H has diagonal entries p and p and symmetric off-diagonal entries q then the matrix H has eigenvalues $p + q$ and $p - q$ and so is positive definite if $p > q$. In the case of the triangle in Figure 1 assuming that x and y are in the horizontal and vertical directions respectively, the values of d_i for this matrix are

$$d_1 = ph_1^2 \ , \ d_2 = \alpha^2 h_1^2 (p(1 + \mu_1^2) - 2\mu_1 q) \ and \ d_3 = \alpha^2 h_1^2 (p(1 + \mu_2^2) - 2\mu_2 q), \tag{10}$$

where

$$\mu_1 = (1 - \beta)/\alpha, \ \text{and} \quad \mu_2 \ = \ \beta/\alpha.$$

In this case d_2 and d_3 can be negative if both p and q are positive and $q \gg p$. It is also possible to pick α and μ_1 so that $d_1 + d_2 + d_3 = 0$ in this case and hence make zero part of equation (9).

The importance of Nadler's error estimate [36], as described in this section is that it enables the connection between the error, the element shape and solution derivatives to be clearly seen.

4 A Mesh Quality Indicator for Linear Triangular Elements

In this section the new mesh quality indicator of Berzins [16] based on the work of Nadler [36] will be described. This indicator takes into account both the geometry and the

solution behaviour. The starting point for this indicator is equation (9). In the case when the values of d_i are all equal then each edge makes an equal contribution to the error. However in order to take into account in a consistent way the fact that the values of d_i may be of different signs it is necessary to consider their absolute values. It should also be noticed that if $d_i = h_i$ then the form of equation (9) has some similarities with the indicators of Bank [12] and Weatherill [48]. This relationship will be made precise below. With these two points in mind the scaled forms of the derivatives d_i are defined by

$$\tilde{d_i} = \frac{|d_i|}{d_{max}} \text{ where } d_{max} = max\left[|d_1|, |d_2|, |d_3|\right] . \tag{11}$$

For notational convenience define

$$\tilde{q}(\underline{\tilde{d}}) = (\tilde{d_1} + \tilde{d_2} + \tilde{d_3})^2 + \tilde{d_1}^2 + \tilde{d_2}^2 + \tilde{d_3}^2 \tag{12}$$

where $\underline{\tilde{d}} = [\tilde{d_1}, \tilde{d_2}, \tilde{d_3}]^T$. A measure of the anisotropy in the derivative contributions to the error is then provided by

$$q_{aniso} = \frac{\tilde{q}(\underline{\tilde{d}})}{12} . \tag{13}$$

The definitions of the coefficients $\tilde{d_i}$ in equation (11) result in the bounds

$$\frac{1}{6} \leq q_{aniso} \leq 1 . \tag{14}$$

Consider a triangle with only one edge contributing to the error. In this case $q_{aniso} = 1/6$ whereas if two edges contribute equally and the third makes no contribution $q_{aniso} = 1/2$.

In order to derive a consistent and related but geometry-only based indicator it should be observed that the quantity defined by:

$$q_m(\underline{h}) = \frac{\tilde{q}(\underline{h})}{16\sqrt{3}\ A}$$

where $\underline{h} = [h_1, h_2, h_3]^T$, has value 1 for an equilateral triangle and tends to the value infinity as the area of a triangle tends to zero but at least one of its sides is constant. It is now possible to explain the relationship between this indicator and those of Bank [12] and Weatherill [48] as denoted by q_b and q_w and defined by

$$\frac{1}{q_b} = \frac{1}{4\sqrt{3}\ A}\left[h_1^2 + h_2^2 + h_3^2\right], \quad q_w = \frac{1}{3\ A}\left[(h_1 + h_2 + h_3)^2\right] \tag{15}$$

respectively. Hence,

$$q_m(\underline{h}) = \frac{1}{4\ q_b} + q_w \frac{\sqrt{3}}{16} . \tag{16}$$

The relationship between q_{aniso} and the linear interpolation error is that when the matrix H is positive definite, i.e. $d_i > 0$, then

$$q_{aniso} = \frac{15}{A\ d_{max}^2} \int_T (e_{lin}(x,y))^2 dx\ dy, \tag{17}$$

thus showing that the indicator is a scaled form of the interpolation error in this special case.

4.1 Edge Indices and Hessian-Based Mesh Movement.

In the case when q_{aniso} is small then it is possible to define an edge index which indicates how much each edge contributes to the error. Suppose that in equation (12) all the values of the terms $\tilde{d}_i$ are identical, say, $\tilde{d}_{avg}$ then

$$\tilde{q}(\tilde{d}) \;=\; 12(\tilde{d}_{avg})^2 \tag{18}$$

Hence

$$\tilde{d}_{avg} \;=\; \sqrt{q_{aniso}} \tag{19}$$

The edge index for each edge is then denoted by $e_{ind}(i)$ and defined by

$$e_{ind}(i) \;=\; \frac{\tilde{d}_i}{\tilde{d}_{avg}}, \quad i = 1, 2, 3. \tag{20}$$

These edge indices thus indicate which edges should be refined to reduce the error. One recent method to take advantage of such local gradients is the modified Delaunay approach of Borouchaki et al. [20] in which the local gradient information, of the form of d_i values, is used in conjunction with the Delaunay mesh generator to compute highly stretched grids for anisotropic flows in two space dimensions. The results presented by Borouchaki et al. show that this approach can give good results on problems with highly directional flows. Similar approaches to generating stretched meshes have been used for some time for highly-directional aerospace problems by practitioners such as Mavriplis [33], although the stretching criteria have usually been derived from physical quantities rather than the error directly.

The work of Peraire et al., [39], used directions based on the eigenvalues of the Hessian matrix as a basis for generating the underlying mesh. This approach was developed into the recent mesh movement method of Ait-Ali-Yahia et al. [2] and Dolejsi [24]. A common feature of all of these methods is that the Hessian matrix is used as a basis for realigning the mesh. This Hessian matrix, H, is modified to be positive definite and edge indicators, defined in the notation used here by $d_i/\sqrt{\Delta x_i^2 + \Delta y_i^2}$, are used to move the mesh. This approach thus scales the edge error component by the edge length. Ait-Ali-Yahia et al. [2] interpret d_i as the edge length in the metric based on the Hessian matrix. The scaling defined by equation (20), in contrast, scales $|d_i|$ by an averaging factor taken over all the edges in the triangle. In the case when H is not positive definite, as in Example 2 of Section 2 if the original values of d_2 and d_3 are negative (i.e. $q > p$), then the effect of the approach of Ait-Ali-Yahia et al. [2] is to transpose q and p in the H matrix and hence in the definitions of d_1, d_2 and d_3 thus giving different values from those in Section 2:

$$d_1 = qh_1^2 \;,\; d_2 = \alpha^2 h_1^2 (q(1+\mu_1^2) - 2\mu_1 p)$$

$$\text{and} \quad d_3 = \alpha^2 h_1^2 (q(1+\mu_2^2) - 2\mu_2 p),$$

where μ_1 and μ_2 are defined as in Example 2 of Section 2. The modified Hessian thus corresponds to the function $\frac{1}{2}\left(qx^2 + 2pxy + qy^2\right)$ and the difference between these functions is $\frac{1}{2}(p-q)\;(x-y)^2$. The key quantities for mesh stretching, the eigenvalues and eigenvectors of the Hessian matrix remain unchanged, however.

Very recently Kunert [31] has conducted a theoretical study that shows that the Hessian strategy produces anisotropic meshes that are well aligned with the solution. By

using his previous results on the Poisson equation [28, 29, 30] Kunert shows that the error in the energy norm is bounded from both above and below. For example he shows that

$$||e_{lin}(x,y)||^2_{H^1(T)} \leq m_1 \left[\sum \eta^2 + \sum \xi^2\right]^{\frac{1}{2}} \tag{21}$$

where η is a local error estimator on an element and where ξ relates to the approximation error of the data. The quantity m_1 is the so called matching function whose presence is due to the anisotropic mesh. Kunert also shows under some heuristic assumptions that the Hessian based approach results in a matching function bounded above by a constant and that as a consequence reliable and efficient error estimation is possible and that the practical success [3, 21] of the Hessian approach is due to the underlying theoretical soundness of the approach.

4.2 Boundary Layer Flow Example

The performance of the q_{aniso} indicator may be illustrated by considering anisotropic flow, such as that in a viscous boundary layer, in which the three triangles defined as Case(a), Case(b) and Case(c) in Figure 2 are used to model a flow with a weak horizontal component $u_{xx} = 1$, an intermediate cross derivative $u_{xy} = 100$ and and a strong vertical component $u_{yy} = 10000$. Case(a) is representative of a triangle thought to be especially suitable for such flows while Case(b) is closer to the type of triangles produced by unstructured mesh generators. Table 1 shows the values of q_{aniso} for the three triangles as the height of the triangles α is varied. Also shown is the ratio of the L_2 errors for Case (a) and Case (b) divided by the error in Case(c). The table shows that in the case when $\alpha < 0.04$ triangles such as that in Case(b) are best in terms of interpolation error and that when $\alpha > 0.04$ triangles such as that in Case(c) are best in terms of interpolation error. The values of the mesh anisotropy indicator q_{aniso} show how the error is distributed and that smaller values of this indicator seem preferable since then one or more edges are aligned with the flow. For very small values of α anisotropy is not a key factor as the dominant flow direction is then the horizontal one and not the vertical one.

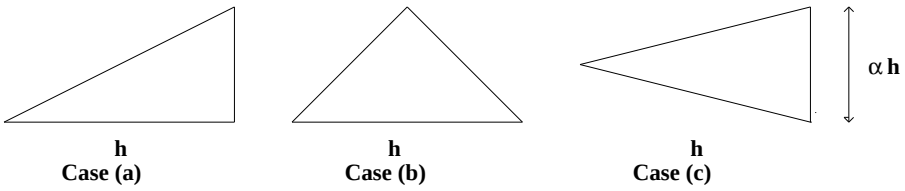

Figure 2: Boundary layer flow example triangles.

4.3 Choice of Norm

Berzins [17], shows that when the same example as in Section 4.2 is considered the error ratios, unlike those in Table 1, vary with the aspect ratios of the triangles. The following example will illustrate how the choice of norm may be critical in deciding what is the best mesh by considering the $H^1(T)$ and $L_2(T)$ norms. The linear interpolation error in the H^1 error norm is defined by equation (2) as $||e_{lin}(x,y)||_{H^1(T)}$. The example used

Table 1: Mesh Anisotropy indicator values

α	Case (a)	Case (b)	Case (c)	Error Ratio a/c	Error Ratio b/c
1.0	0.49	0.49	0.29	1.8	1.70
0.1	0.42	0.42	0.35	1.8	1.40
0.038	0.35	0.34	0.53	1.7	1.00
0.02	0.30	0.29	1.00	1.5	0.71
0.01	0.28	0.30	0.68	1.3	0.44
0.001	0.42	0.29	0.50	1.0	0.47
0.0001	0.49	0.28	0.50	1.0	0.55

is that of Babuska and Aziz [10] in which triangles of the form of that in Figure 1 are used to model a solution, u, with a horizontal component $u_{xx} = 1$ and no other non-zero components: $u_{xy} = 0$ and $u_{yy} = 0$. (In the notation of Babuska and Aziz, [10], their H is αh in Figure 1 and the cases $\beta = 1$ and $\beta = \frac{1}{2}$ are considered.) Hence $U(x, y) = \frac{1}{2}x^2$ and $U_{lin}(x, y) = \frac{1}{2}x + \beta(\beta - 1)y/(2\alpha)$ and so

$$(\frac{\partial}{\partial x}e_{lin}(x, y))^2 \ + \ (\frac{\partial}{\partial y}e_{lin}(x, y))^2 \ = \ (x - \frac{1}{2})^2 \ + \ \beta(\beta - 1)/(2\alpha)^2$$

thus showing a potential source of problems for small values of α. Berzins [16] shows that

$$||e_{lin}(x, y)||^2_{H^1(T)} \ = \ \frac{A}{12}\left[\ \frac{1}{15}\tilde{q}(\underline{d}) \ + \ \tilde{r}(\underline{d}) \ \right] \tag{22}$$

where for this problem

$$\tilde{q}(\underline{d}) = h^4 \left[(1 + \beta^2 + (1 - \beta)^2)^2 + (1 - \beta)^4 + 1 + \beta^4\right], \tag{23}$$

$$\tilde{r}(\underline{d}) = 4h^2 \left[\frac{3\beta^2(1 - \beta)^2}{\alpha^2} + (1 - \beta)^2 + \beta^2\right] \tag{24}$$

and the term $\tilde{q}(\underline{d})$ is defined in equation (12). These results are interesting because they show that in the L_2 norm $\beta = \frac{1}{2}$ is more accurate whereas in the H^1 norm for $\alpha < 0.4629$, $\beta = 1$ or $\beta = 0$ is more accurate and $\beta = 0.5$ is the worst value as $\alpha \downarrow 0$. Hence a good mesh in one norm may not be a good mesh in another norm.

4.4 Non-Quadratic Functions

The extension to the case of non-quadratic functions may be considered by assuming that the exact solution is locally quadratic. Bank [11, 12] uses such an approach inside the code PLTMG and calculates estimates of second derivatives. Adjerid, Babuska and Flaherty [1] use a similar approach based on derivative jumps across edges to estimate the error. An alternative approach is to use the ideas of Hlavacek et al. [26] to estimate nodal derivatives and hence second derivatives.

5 Linear Tetrahedral Approximation of Quadratics

Although there are now data-dependent tetrahedralisations, see Nielson [38], there are unfortunately very few error estimates for tetrahedral meshes that show the explicit dependence of the error on the mesh and the solution. The natural starting point is perhaps

to try to use the interpolation error to assess how appropriate the mesh is for the computed solution. The simple mesh quality indicator of Berzins [16, 17] is based on linear interpolation L_2 error estimates and is derived by extending Nadler's [36] approach to tetrahedra by considering the case in which a quadratic function

$$u(x,y,z) \;=\; \frac{1}{2}\,\underline{x}^T\; H\; \underline{x} \text{ where } \quad \underline{x} \;=\; \begin{bmatrix} x \\ y \\ z \end{bmatrix} \tag{25}$$

is approximated by a linear function $u_{lin}(x,y,z)$ defined by linear interpolation based on the values of u at the vertices of a tetrahedron T defined by the vertices $\underline{v}_1, \underline{v}_2, \underline{v}_3$ and $\underline{v}_4$ as shown in Figure 3a.

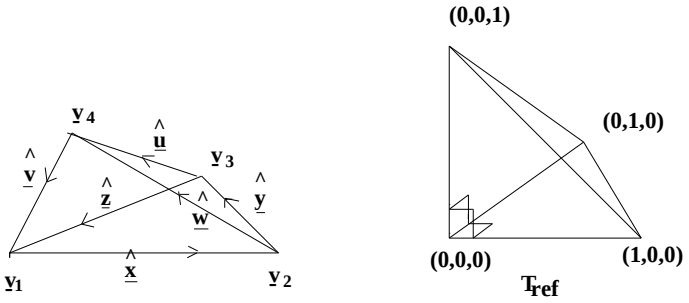

Figure 3: (a) Example tetrahedron and (b) reference tetrahedron.

Let h_i be the length of the edge connecting $\underline{v}_i$ and $\underline{v}_{i+1}$ where $\underline{v}_5 = \underline{v}_1$. With reference to Figure 3a define the vectors $\underline{\hat{x}}$, $\underline{\hat{y}}$, $\underline{\hat{z}}$, $\underline{\hat{u}}$, $\underline{\hat{v}}$ and $\underline{\hat{w}}$ by

$$\begin{aligned} &\underline{v}_2 = \underline{v}_1 + \underline{\hat{x}}, \quad \underline{v}_3 = \underline{v}_2 + \underline{\hat{y}}, \quad \underline{v}_1 = \underline{v}_3 + \underline{\hat{z}} \\ &\underline{v}_4 = \underline{v}_1 - \underline{\hat{v}}, \quad \underline{v}_4 = \underline{v}_2 + \underline{\hat{w}}, \quad \underline{v}_4 = \underline{v}_3 + \underline{\hat{u}} \end{aligned} \tag{26}$$

and consequently

$$\underline{\hat{x}} + \underline{\hat{y}} + \underline{\hat{z}} \;=\; \underline{\hat{x}} + \underline{\hat{w}} + \underline{\hat{v}} \;=\; \underline{\hat{u}} + \underline{\hat{v}} - \underline{\hat{z}} \;=\; 0. \tag{27}$$

Define a reference tetrahedron T_{ref}, see Figure 3b, by the four nodal points:

$$\underline{v}_1 = (0,0,0)^T \;\;,\;\; \underline{v}_2 = (1,0,0)^T \;\;,\;\; \underline{v}_3 = (0,1,0)^T \;\;,\;\; \underline{v}_4 = (0,0,1)^T \;. \tag{28}$$

Then the mapping from the tetrahedron, T_{ref}, to the tetrahedron, T is given by

$$\underline{x} = \underline{v}_1 \;+\; B\;\underline{\tilde{x}} \tag{29}$$

where $B \;=\; [\underline{\hat{x}}, -\underline{\hat{z}}, -\underline{\hat{v}}]$, $\underline{\tilde{x}}$ is in the reference tetrahedron, T_{ref}, and $\underline{x}$ is the equivalent point in the original tetrahedron T.
The function u may then be expressed as

$$u(x,y,z) \;=\; \frac{1}{2}\;v_1^T\;H\;v_1 \;+\; \frac{1}{2}\;\underline{\tilde{x}}^T\;B^T\;H\;v_1 \;+\; \frac{1}{2}\;v_1^T\;H\;B\;\underline{\tilde{x}} \;+\; \frac{1}{2}\;\underline{\tilde{x}}^T\;B^T\;H\;B\;\underline{\tilde{x}} \tag{30}$$

where $\underline{\tilde{x}} \;=\; [x,y,z]^T$, is defined on T_{ref}. Ignoring the constant and linear terms (which are approximated exactly by a linear interpolant) and expanding the remaining quadratic term using equation (29) gives

$$\begin{aligned} u(x,y,z) \;=\; \frac{1}{2}\;[&(\underline{\hat{x}}^T H \underline{\hat{x}})x^2 + (-\underline{\hat{x}}^T H \underline{\hat{z}})2xy + (\underline{\hat{z}}^T H \underline{\hat{z}})y^2 \\ &(-\underline{\hat{x}}^T H \underline{\hat{v}})2xz + (\underline{\hat{z}}^T H \underline{\hat{v}})2zy + (\underline{\hat{v}}^T H \underline{\hat{v}})z^2 \;\;]\;. \end{aligned}$$

Interpolating this by a linear function defined on T_{ref} by the nodal solution values gives

$$u_{lin}(x,y,z) \;=\; \frac{1}{2}\;\left[(\underline{\hat{x}}^T H\underline{\hat{x}})x + (\underline{\hat{z}}^T H\underline{\hat{z}})y + (\underline{\hat{v}}^T H\underline{\hat{v}})z\;\right] \tag{31}$$

and hence the linear interpolation error may be defined as:

$$e_{lin}(x,y,z) = u(x,y,z) \;-\; u_{lin}(x,y,z)\;. \tag{32}$$

Berzins [16] shows that this may then be written as

$$\int_T\;(e_{lin}(x,y,z))^2 dx\;dy\;dz = \;\frac{3}{2}\;V\;\underline{d}^T\;P\;\underline{d} \tag{33}$$

where V is the volume of the tetrahedron, the vector of second directional derivatives along edges is defined by

$$\underline{d}^T = \frac{1}{2}\;[d_1,...,d_6\;] \;=\; \frac{1}{2}\;\left[\underline{\hat{x}}^T H\underline{\hat{x}},\;\;\underline{\hat{y}}^T H\underline{\hat{y}},\;\;\underline{\hat{z}}^T H\underline{\hat{z}},\;\;\underline{\hat{u}}^T H\underline{\hat{u}},\;\;\underline{\hat{v}}^T H\underline{\hat{v}},\;\;\underline{\hat{w}}^T H\underline{\hat{w}}\;\right]$$

and the matrix P is defined by

$$P \;=\; \frac{4}{7!}\;\begin{bmatrix} 4 & 2 & 2 & 1 & 2 & 2 \\ 2 & 4 & 2 & 2 & 1 & 2 \\ 2 & 2 & 4 & 2 & 2 & 1 \\ 1 & 2 & 2 & 4 & 2 & 2 \\ 2 & 1 & 2 & 2 & 4 & 2 \\ 2 & 2 & 1 & 2 & 2 & 4 \end{bmatrix}.$$

Expanding out equation (33) in terms of the components of $\underline{d}$, which are the six directional derivatives along the edges, gives:

$$\int_T\;(e_{lin}(x,y,z))^2 dx\;dy\;dz = \;\frac{6}{4}\;V\;\frac{8}{7!}\;\left[(\Sigma d_i)^2 - d_1d_4 - d_2d_5 - d_3d_6 + \Sigma d_i^2\;\right]\quad. \tag{34}$$

6 Tetrahedral Mesh Quality Indicator

The results in the previous section make it possible to define a mesh quality indicator in the same way as in Section 4 in that the error is scaled by the maximum directional derivative d_{max} and the integral is scaled by the volume before taking the square root. In a similar way to that found in Section 4 define

$$\tilde{Q}(\underline{\tilde{d}}) \;=\; \left[(\Sigma\tilde{d}_i)^2 - \tilde{d}_1\tilde{d}_4 - \tilde{d}_2\tilde{d}_5 - \tilde{d}_3\tilde{d}_6 + \Sigma\tilde{d}_i^{\,2}\;\right] \tag{35}$$

where now $\underline{\tilde{d}} = [\tilde{d}_1,\tilde{d}_2,\tilde{d}_3,\tilde{d}_4,\tilde{d}_5,\tilde{d}_6]^T$. A measure of the anisotropy in the derivative contributions to the error is then provided by

$$Q_{aniso} \;=\; \frac{\tilde{Q}(\underline{\tilde{d}})}{39}\;. \tag{36}$$

By adopting a similar approach to that used in Section 4 a geometry based indicator can be written as

$$Q_m(\underline{h}) = \frac{C}{V}\;\left[\;\tilde{Q}(\underline{\tilde{h}})\right]^{\frac{3}{2}} \tag{37}$$

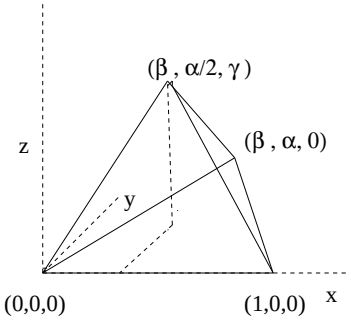

Figure 4: Example anisotropic tetrahedron

where C is a scaling factor to ensure that the indicator has value one when $h_i = h$ and thus $C = 1/(8.48528 \times 39^{1.5})$ and the power of $\frac{3}{2}$ reflects the different dimensions of the error and the volume in powers of h. The edge quality estimator used by Weatherill [48] Q_w is defined by equation(6). A comparison of these two indicators on tetrahedra with uniform gradients was done by Berzins [16] using the eight parameterised tetrahedra of Liu and Joe [32] as defined by Figures 4 to 11 of that paper and showing that the values of the two indicators differ by less than ten percent but on rare occasions that this difference may rise to 25 percent.

6.1 Edge Indices

As in two dimensions it is possible to define an edge index which indicates how much each edge contributes to the error. Suppose that in equation (35) all the values of $\tilde{d}_i$ are identical, say, $\tilde{d}_{avg}$ then

$$\tilde{Q}(\underline{\tilde{d}}) = 39(\tilde{d}_{avg})^2 \ . \tag{38}$$

Hence

$$\tilde{d}_{avg} = \sqrt{Q_{aniso}} \quad . \tag{39}$$

The edge index for each edge is then denoted by $e_{ind}(i)$ and defined by

$$e_{ind}(i) = \frac{\tilde{d}_i}{\tilde{d}_{avg}}, \quad i = 1, 2, 3, 4, 5, 6. \tag{40}$$

6.2 Anisotropic Tetrahedra

In order to consider the case when the edge derivatives are nonuniform consider the model tetrahedron in Figure 4 defined by the four points

$$\underline{x}_1 = [0, 0, 0]^T \ , \ \underline{x}_2 = [1, 0, 0]^T, \ \underline{x}_3 = [\beta, \alpha, 0]^T \text{ and } \ \underline{x}_4 = [\beta, \frac{\alpha}{2}, \gamma]^T$$

with edge lengths

$$h_1 = 1, h_2 = \sqrt{\alpha^2 + (1-\beta)^2}, \quad h_3 = \sqrt{\alpha^2 + \beta^2},$$

$$h_4 = \sqrt{\alpha^2/4 + \gamma^2}, \ h_5 = \sqrt{\alpha^2/4 + \beta^2 + \gamma^2}, \text{ and } h_6 = \sqrt{\alpha^2/4 + (1-\beta)^2 + \gamma^2}.$$

The volume of this tetrahedron is given by V where $V = \alpha\gamma/6$. The anisotropy of the solution, $u = \frac{1}{2}x^2$, is shown by the fact that the directional derivatives d_i given below depend only on β and not on γ or α.

$$d_1 = 1/2, d_2 = 1/2(1-\beta)^2, d_3 = 1/2\beta^2,$$

$$d_4 = 0,\ d_4 = 1/2\beta^2,\ \text{and}\ d_6 = 1/2(1-\beta)^2.$$

Given these definitions the anisotropy indicator has the value shown in the table below. In contrast a geometry based indicator such as that of Weatherill, will for small values of α and β indicate a possible source of problems, as is shown in Table 2 below. Table 2 also shows the values of the $H^1(T)$ norm which is defined as in Section 1 except that there is now a third gradient term $(\frac{\partial}{\partial z}e_{lin}(x,y))^2$ and the gradient terms sum to

$$\int_T (\frac{\partial}{\partial x}e_{lin}(x,y,z))^2 + (\frac{\partial}{\partial z}e_{lin}(x,y,z))^2 + (\frac{\partial}{\partial z}e_{lin}(x,y,z))^2 dxdydz \ = \\ \frac{V}{4} \ \times \left[0.05 + 1.2(\beta - 0.5)^2 + \beta^2(1-\beta)^2(\frac{1}{\alpha^2} + \frac{1}{\gamma^2})\right]. \tag{41}$$

Hence as in Section 4.3 this norm is sensitive to small values of α and/or γ. Yet again the behaviour of the error norms exhibits different trends from the indicator Q_w. Thus again suggesting that the error norm be used to identify which elements should be refined and the anisotropy indicator and the values of d_i to determine which edges should be selected for refinement. In Table 2 the L_2 and H^1 norms for each value of $\beta = 0.0, 0.5$ are scaled by the value of the norm when $\alpha = \gamma = 1$. This makes a comparison with the mesh quality indicator Q_w easier as it has a values close to 1 at these points.

Table 2: Comparison of Q_{aniso}, Q_w and Square of L_2 and H^1 Norm Values

		$\beta = 0$			$\beta = 0.5$		
Indicator	α/γ	0.01	1.0	100.0	0.01	1.0	100.0
Q_{aniso}		0.28	0.28	0.28	0.12	0.12	0.12
Q_w	0.01	9.1e+2	5.2e+1	9.0e+4	8.9e+2	4.7e+1	9.0e+4
	1.00	5.5e+1	1.20	9.1e+2	4.5e+1	1.03	9.1e+2
	100.	1.4e+5	1.4e+3	5.0e+1	1.4e+5	1.4e+3	5.1e+1
Scaled	0.01	1.0e-4	1.0e-2	1.0	1.0e-4	1.0e-2	1.0
L_2^2	1.00	1.0e-2	1.0	1.0e+2	1.0e-2	1.0	1.0e+2
error	100.	1.0	1.0e+2	1.0e+4	1.0	1.0e+2	1.0e+4
Scaled	0.01	1.0e-4	1.0e-2	1.0	6.9e-1	3.5e+1	3.5e+3
$(H^1(T))^2$	1.00	1.0e-2	1.0	1.0e+2	3.5e+1	1.0	6.5e+1
error	100.	1.0	1.0e+2	1.0e+4	3.5e+3	6.5e+1	3.0e+3

The indicators Q_w , Q_{aniso} and the L_2 error are symmetric about $\beta = 0.5$. In particular when α and γ are small then $h_i \approx d_i$ and

$$Q_w = \frac{1}{8.48528V} \ \left[(\Sigma\frac{d_i}{6})^3\right] \ . \tag{42}$$

Hence as the volume shrinks the mesh quality indicator Q_w becomes large while the approximation error for a fixed value of β is scaled only by the volume. The most significant result is that the indicator Q_{aniso} doesn't vary with α and γ and the error norm naturally increases as α, γ, and hence the volume, get large. In contrast the mesh quality indicator Q_w has a minimum when $\alpha = \gamma = 1$ and is also relatively small when α and γ are large and the error is also large. Table 3 shows the values of the indicator if 1 to 6 edges are active in that they have equal values of the edge gradients d_i and the remaining edges have zero values of d_i. The variation in the values of Q_d takes into account different permutations of zero and non-zero values of d_i. The table thus provides a way of understanding the meaning of the values produced by the indicator.

Table 3: Interpretation of Q_d Values

Edges Active	1	2	3	4	5	6
$Q_(d)$	2	5-6	9-12	19-22	27-28	39
$Q_(d)/40$	1/20	1/8	1/4	1/2	7/10	1

7 Laplace and Poisson Equation Examples in 3D

The issue of mesh suitability for a given solution and numerical solver is recognised as a complex one with no easy answers. There are a variety of views concerning the sensitivity of numerical schemes to distorted meshes. Shephard [45] states that the stabilised FEM for example, appears to have no real problem with elements with angles close to 180 degrees and very large aspect ratios and that tetrahedra with small angles are well-understood to be needed for boundary layer calculations. In contrast, Millar et al. [34, 35], state that for Laplace's equation, finite volume schemes are less sensitive than finite element schemes to sliver-type tetrahedra in meshes. Given the similarity between the finite volume and element schemes in this case, see [13], the difference may be due to implementation issues such as those discussed by Putti and Cordes [40].

Apel et al. [4, 8] describe some of the deeper theoretical issues to do with the Poisson equation, $-\Delta u = f$ in Ω, with Dirichlet boundary conditions, $u = g$ on $\partial\Omega$, in a polyhedral domain $\Omega \subset R^3$. The solution to this problem u behaves anisotropically due to singularities of r^λ type near edges with interior angle ω, with $\lambda = \pi/\omega < 1$ for $\omega > \pi$, where r is the distance to the edge. As a result of this singularity, the finite element method with piecewise linear shape functions on a quasi-uniform family of tetrahedral meshes converges with order h^λ in the energy norm. To recover the optimal convergence order h, an anisotropically refined finite element mesh is used by Apel [5]. Apel et al, [4] also state that despite more research into error estimators for anisotropic meshes there are few rigorously analyzed error estimators. Some strictly mathematically-based estimators have appeared recently however, due to Siebert [42], Kunert [28, 29], Kunert and Verfürth [30] and Dobrowolski et al. [23]. Even so, [4], the theory of these estimators is not as complete as for isotropic elements since, at this time, no local error estimator is known that bounds the error reliably from *above and below*, independently of the mesh $\mathcal{T}_h$ and the solutions u and u_h. In other words, the effectivity index cannot be guaranteed to be $\mathcal{O}(1)$.

In order to understand better the dependency between the mesh and the error, the Laplace equation, $\nabla^2 U = 0$, in three space dimensions of [34] will be used in two simple examples.

7.1 Example 1

In the first case, the mesh of five points consists of a single tetrahedron sub-divided into four by the addition of an internal point and is shown in Figure 5. The analytic solution is given by

$$u(x, y, z) = e^{\pi z} cos(\pi y/\sqrt{2}) sin(\pi(x + 0.5)/\sqrt{2}) \tag{43}$$

where the points O, A, B, C, D and E are defined by:

$$O = [0, 0, 0]^T,\ A = -[0.5, 0.5, 0]^T,\ B = [0.5, -0.5, 0]^T$$

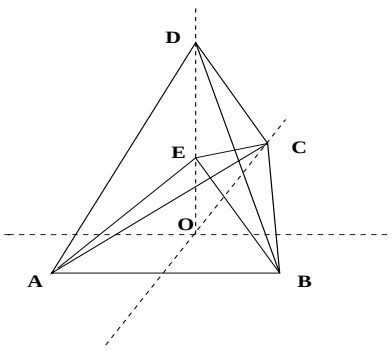

Figure 5: Example mesh of four tetrahedra: ABCE,ABED,ACED and BCED

$$C = [0, 1, 0]^T,\ D = [0, 0, 1]^T,\ \text{and}\ \ E = [0, 0, \epsilon]^T$$

where ϵ is a parameter that will be varied to test the sensitivity of the numerical solution to the mesh and in particular to distorted elements. The values at A, B, C, D are given by the exact solution and denoted by U_A, U_B, U_C, U_D and so only U_E needs to be calculated. The scheme used to approximate the Laplacian is Barth's cell-vertex scheme [13, 14]. This gives a challenging situation for mesh quality indicators as the region associated with each node is composed of parts of all neighbouring tetrahedra. At point E the Laplacian is approximated by

$$\begin{aligned}\nabla^2 U = W_{EA}(U_A - u_E) + W_{EB}(U_B - u_E) + \\ W_{EC}(U_C - u_E) + W_{ED}(U_D - u_E)\end{aligned} \tag{44}$$

where the coefficients W_{**} are defined by Barth [13, 14], u_E is the numerical approximation to the exact value U_E and is explicitly defined by the equation

$$\begin{aligned}u_E = (W_{EA}U_A + W_{EB}U_B + W_{EC}U_C + W_{ED}U_D)/ \\ (W_{EA} + W_{EB} + W_{EC} + W_{ED})\end{aligned} \tag{45}$$

In order that the solution satisfies a maximum principle all the weights W_{**} must be positive, [13, 14]. Barth also shows how this condition may not be met on a distorted mesh, but Putti and Cordes [40] show how to modify the method to avoid this and that this also improves the accuracy. This issue is of critical importance in some practical applications because the computation of non-physical negative values may cause the calculation to fail.

Denote the exact solution of the problem at node E by U_E then the p.d.e. truncation error, T_{Err}, is defined by

$$\begin{aligned}T_{Err} = W_{EA}(U_A - U_E) + W_{EB}(U_B - U_E) + \\ W_{EC}(U_C - U_E) + W_{ED}(U_D - U_E)\end{aligned} \tag{46}$$

and the relationship between the truncation error and the error at point E, $Error = U_E - u_E$ is

$$U_E - u_E = -\frac{T_{Err}}{(W_{EA} + W_{EB} + W_{EC} + W_{ED})}. \tag{47}$$

Table 4 shows the different mesh quality indicators and the interpolation error as the value of ϵ changes for two tetrahedra given by the points ABCE and ACED. The values for the tetrahedra ABED and BCED being similar to those of ACED. With reference to Table 4, Interp is the square of the interpolation error based on the exact solution. In Table 5, Err and T.Err are the error and truncation error defined by equations (47) and

Table 4: Q_{aniso} and Standard Mesh Quality Q_w

	Tet. ABCE			Tet. ACED		
ϵ	Q_{aniso}	Q_w	Interp	Q_{aniso}	Q_w	Interp
0.001	0.35	621	3.4e-6	0.15	2.2	1.0e-3
0.01	0.35	62	3.4e-5	0.15	2.2	1.0e-3
0.5	0.38	1.5	1.6e-3	0.17	3.9	6.2e-4
0.99	0.21	1.1	3.6e-3	0.22	211	2.0e-5
0.999	0.20	1.1	3.6e-3	0.23	211	2.1e-6

Table 5: Solution Error Values

	Numerical Error		
ϵ	U_E	Err	T. Err
0.001	-2.6e-2	0.42	-107.
0.01	-1.7e-2	0.41	-11.4
0.5	5.2e-1	0.01	-0.65
0.99	1.07	3.2e-3	-0.07
0.999	1.08	2.8e-5	-0.06

(46) respectively. The results in Table 4 show that the anisotropy indicator follows (not surprisingly) the trend of the interpolation error, but that the pointwise discretization error behaves very differently, especially for small values of ϵ. The low values of the anisotropy indicator Q_{aniso} indicate potential problems. The geometry indicator does a good job of picking up the very large error for small ϵ on element ABCE but also erroneously identifies a problem on element ACED when ϵ is close to one and the error is small.

The interesting result is that both mesh quality indicators do not really identify the relationship between the mesh and the error in the numerical solution. Part of the reason for this is that the volume used by the discretisation method to define the residual at a node is the sum of parts of the volumes of the individual tetrahedra surrounding that node. It is the differing size of the truncation error as caused by the method coefficients that has a dramatic effect on the error. In the case when $\epsilon = 0.001$ the large value of the coefficients W_{ea} and W_{eb}, W_{ec} arise because the face angle between faces such as EBC and ABC is very close to π. Hence in this case the value U_D plays little part in determining u_E. In contrast when ϵ is close to one only one coefficient is large and u_E is determined almost solely by U_D its closest neighbour. The values of the coefficients W_{eb} and W_{ed} etc, are shown in Table 6.

Table 6: Values of the coefficients $W_{ea}, W_{eb}, W_{ec}, W_{ed}$

ϵ	W_{ea}, W_{eb}, W_{ec}	W_{ed}
0.001	8.0e+1	2.52e-1
0.01	9.0	2.72e-1
0.5	8.3e-1	2.5
0.99	7.5e-1	2.2e+2
0.999	7.5e-1	2.4e+3

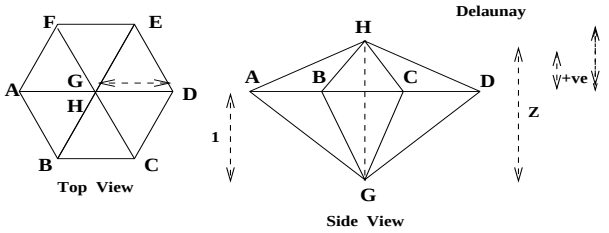

Figure 6: Barth's Example Mesh to demonstrate non-positivity

Table 7: Error Variation with z variation in Barth's Example.

z	E_{Barth}	E_{Putti}	Q_{aniso}	Q_w
0.25	0.07	0.08	0.42	4.3
0.50	0.19	0.25	0.40	2.1
1.00	0.32	0.41	0.34	1.2
1.25	0.22	0.21	0.30	1.1
1.50	0.35	0.01	0.26	1.1
1.80	0.18	0.12	0.31	1.1
2.00	0.29	0.15	0.40	1.2
2.50	0.51	0.06	0.48	1.5
3.00	0.67	3.30	0.40	1.8

7.2 Example 2

In the second case consider the simple mesh of 6 tetrahedra used by Barth [13] to demonstrate that a linear tetrahedral finite element solution on a Delaunay mesh may give a solution with the wrong sign. The mesh in Figure 6 is parameterised by the position of node H above G as denoted by Z in the diagram. The coordinates of the mesh points are:

$$A = [-1, 0, 0]^T,\ B = [-0.5, -d, 0]^T,\ C = [0.5, -d, 0]^T$$

$$D = [1, 0, 0]^T,\ E = [0.5, d, 0]^T,\ F = [-0.5, d, 0]^T$$

$$G = [0, 0, -1]^T, \text{and}\ \ H = [0, 0, z-1]^T$$

where z is the parameter being varied and $d = \sqrt{3}/2$. As indicated in Figure 6, Barth shows that the mesh is Delaunay for values of $1 < z < 2$ but gives rise to positive coefficients W_{**}(see equation(47)) only if $1 < z < 1.75$. In contrast the discretisation of Putti and Cordes [40] gives rise to positive coefficients W_{**} for $1 < z < 2$. Hence the mesh quality in this case has a dramatic impact on the quality of the solution. As in Example 1 Laplace's equation is solved for the unknown value at H given Dirichlet conditions at all the other mesh points defined by equation (43). Table 7 shows the errors in the values of u at the point H for different values of z. E_{Barth} is the error using the method described by Barth while E_{Putti} is the error when the method of Putti and Cordes is used. The table shows that the Putti and Cordes method can produce a much more accurate result for some Delaunay meshes, but also for non-Delaunay meshes that the original method of Barth [13] can give better accuracy sometimes. The anisotropy indicator shows that the amount of anisotropy present is not great while the geometric mesh quality indicator does not, as expected, reflect the error, e.g. for small values of z.

8 Conclusions

This paper has described some of the issues in trying to identify triangular or tetrahedral elements in which the shape of the elements and the local solution gradients conspire to give a poor approximation to a finite element solution. There are five general conclusions to be drawn from this paper.

- Purely geometric mesh quality indicators do a good job of identifying meshing anomalies.
- The appropriateness of a mesh for a given solution depends on both geometry and solution information.
- Interpolation-based mesh quality indicators give a better insight into how the mesh might need to be stretched, but are no substitute for error estimates which include both solution and geometry effects.
- Such error indicators are particularly needed for strongly directional fluid flows for which highly distorted meshes appear to be very effective, but are often not available.
- The mesh generation requirement must be to allow the user to supply mesh quality measures and to choose anisotropic remeshing options.

Acknowledgements

The author would like to thank Thomas Apel, Peter Jimack and Mark Walkley for reading the manuscript and suggesting numerous improvements.

References

[1] S. Adjerid, I. Babuska and J.E. Flaherty, A posteriori error estimation for the finite element method of lines solution of parabolic problems, Math. Models and Meths. Appl. Sci., (to appear).

[2] D. Ait-Ali-Yahia, W.G. Habashi, A. Tam, M-G. Valet and M. Fortin, A directionally adaptive methodology using an edge based error estimate on quadrilateral grids, Int. Jour. for Num. Meths in Fluids. 1996, **23**, 673–690.

[3] R.C. Almeida, R. Feijoo, Adaptive finite element computational fluid dynamics using an anisotropic error estimator, Computer Methods in Applied Mechanics and Engineering 182, 379-400, Feb. 2000.

[4] Th Apel, M Berzins, P K Jimack, A Plaks, I Tsukerman, M Walkley, Mesh Shape and Anisotropic Elements: Theory and Practice, To appear in Proceedings of MAFELAP 1999, ed. J.R. Whiteman, 2000.

[5] Th. Apel and M. Dobrowolski. Anisotropic interpolation with applications to the finite element method. Computing, 47:277–193, 1992.

[6] Th. Apel and G. Lube. Anisotropic mesh refinement for a singularly perturbed reaction diffusion model problem. Appl. Numer. Math., 26:415–433, 1998.

[7] Th. Apel and F. Milde. Comparison of several mesh refinement strategies near edges. Comm. Numer. Methods Engrg., 12:373–381, 1996.

[8] Th. Apel and S. Nicaise. The finite element method with anisotropic mesh grading for elliptic problems in domains with corners and edges. Math. Methods Appl. Sci., 21:519–549, 1998.

[9] Th. Apel. Anisotropic finite elements: Local estimates and applications. Advances in Numerical Mathematics. Teubner, Stuttgart, 1999.

[10] M. Babuska and J. Aziz, On the Angle Condition in the Finite Element Method, SIAM J. Numer. Anal. **13** 1976, No 2, pp. 214–226.

[11] R. E. Bank, PLTMG: A Software Package for Solving Elliptic Partial Differential Equations. Users Guide 8.0 SIAM Publications Philadelphia 1997.

[12] R.E. Bank and R.K.Smith, Mesh Smoothing Using A Posteriori Error Estimates. SIAM J. Numerical Analysis, 34, 979-997, 1997.

[13] T.J. Barth, Numerical Aspects of Computing Viscous High Reynolds Number Flows on Unstructured Meshes. AIAA Paper 91-0721, 29th Aerospace Sciences Meeting, January 7-10, 1991, Reno Nevada.

[14] T.J. Barth, Aspects of Unstructured Grids and Finite Volume Solvers for the Euler and Navier Stokes Equations. Lecture Notes Presented at the VKI Lecture Series 1994-95.

[15] M. Bern, and D. Epstein, Mesh Generation and Optimal Triangulation, Report CSL 92-1, Xerox Corporation, Palo Alto Research Center, 3333 Coyote Hill Road, Palo Alto, CA 94304.

[16] M. Berzins, A solution-based triangular and tetrahedral mesh quality indicator, SIAM Journal on Scientific Computing 19, 2051-2060, 1998.

[17] M. Berzins, A solution-based H^1 norm triangular and tetrahedral mesh quality indicator, pp. 77-89 in Grid Generation and Adaptive Algorithms, proc. of IMA Workshop on Parallel and Adaptive Methods, Eds M.Bern, J.E.Flaherty and M. Luskin, Vol. 113, IMA Volumes in Mathematics and its Applications, Springer, 1999.

[18] M. Berzins, Mesh Quality: A Function of Geometry, Error Estimates or Both? Engineering with Computers, 1999, 15:236-247.

[19] M.Berzins, Solution-based mesh quality indicators for triangular and tetrahedral meshes, Invited paper to appear in Journal of Computational Geometry and Applications.

[20] M. Borouchaki, M.J.Castro-Diaz, P.L. George, F.Hecht and B.Mohammadi, Anisotropic adaptive mesh generation in two dimensions for CFD, in Numerical Grid Generation in Computational Field Simulations, (eds) B.K.Soni, J.F. Thompson, J. Hauser, P.Eiseman. Published by NSF Center for Computational Field Simulations, Mississippi State University, Mississippi 39762 USA , April 06 ISBN 0-965 1627-02

[21] C.G. Buscaglia and E.A. Dari, Anisotropic Mesh Optimisation and its Application in Adaptivity, Int. Jour. for Numer. Meths. in Eng. 40, 4119-4136, 1997.

[22] G. Carey, Computational Grids - Generation, Adaptation and Solution Strategies, Taylor and Francis, Bristol PA 19007, 1997.

[23] M. Dobrowolski, S. Gräf and C. Pflaum. On a posteriori error estimators in the finite element method on anisotropic meshes. Elec. Trans. Numer. Anal., 8:36–45. 1999.

[24] V. Dolejsi, Anisotropic mesh adaptation for finite volume and finite element methods on triangular meshes. Computer Visual Sci. 1: 165-178, 1998.

[25] P.L. George, H. Borouchaki, Delaunay Triangulation and Meshing- Applications to Finite Elements. Editions Hermes, 8 quai du Marché-Neuf, Paris France, ISBN 2-86601-692-0, 1998.

[26] I.Hlavacek, M. Krizek and V.Pistora, How to recover the gradient of linear elements on nonuniform triangulations, Applications of Mathematics 41 1996, 4, 241–267.

[27] M. Krizek, On the maximum angle condition for linear tetrahedral elements, SIAM J. Numer. Anal. 29 1992, 2, 513–520.

[28] G. Kunert. A posteriori error estimation for anisotropic tetrahedral and triangular finite element meshes. Ph.D. Thesis, TU Chemnitz, Germany, 1999. (http://www.tu-chemnitz.de/pub/1999/0012/index.html).

[29] G. Kunert. An a posteriori residual error estimator for the finite element method on anisotropic tetrahedral meshes. To appear in Numerische Mathematik, 2000.

[30] G. Kunert and R. Verfürth. Edge residuals dominate a posteriori error estimates for linear finite element methods on anisotropic triangular and tetrahedral meshes. To appear in Numerische Mathematik, 2000.

[31] G. Kunert. Anisotropic mesh construction and error estimation in the finite element method. Technische Universitat Chemnitz, Preprint-Reihe des Chemnitzer SFB 393/00-01, 2000.

[32] A. Liu and B. Joe, Relationship between tetrahedron shape measures, BIT, 34, 1994, 268–287.

[33] D.M. Mavriplis, Adaptive Mesh Generation for Viscous Flows Using Delaunay Triangulation. Jour. of Computational Physics, 90, 271-291, 1990.

[34] G.L. Millar, D. Talmor, S.H. Teng, N. Walkington, A Delaunay Based Numerical Method for Three Dimensions: generation, formulation and partition. 683-692 in Proc 27th ACM Symposium Theory of Computing '95, Las Vegas, USA. ACM Publications, New York, 1996.

[35] G.L. Millar, D. Talmor, S.H. Teng, N. Walkington, H. Wang. Control Volume Meshes using Sphere Packing- generation, refinement, and coarsening. In the 5th International Meshing Roundtable, 47–61, 1996.

[36] E. J.Nadler, Piecewise linear best L_2 approximation on triangles, in C.K.Chui, L.L.Schumacher and J.D. ward (Eds) Approximation Theory V: Proceedings Fifth International Symposium on Approximation Theory. Academic Press New York 1986, 499–502.

[37] E. J.Nadler, Piecewise linear approximation on triangulations of a planar region, M.Sc. Thesis, Division of Applied Mathematics, Brown University, Providence, RI, May 1985.

[38] G.M.Nielson, Tools for Triangulations and Tetrahedralisations and Constructing Functions Defined over Them. Scientific Visualisation - Overviews,Methodologies and Techniques. eds. G.M.Nielson, H.Hagen and H.Muller E.J.Nadler., IEEE Computer Society, Los Alamitos , California, 1997.

[39] J. Peraire, M. Vahdati, K. Morgan and O.C. Zienkiewicz, Adaptive Remeshing for Compressible Flow Calculations. J. of Comp. Physics, 22, 131-149,1986.

[40] M. Putti and C. Cordes, Finite Element Approximation of the Diffusion Operator on Tetrahedra, SIAM Jour. on Sci. Comput. 19, 1154-1168, 1998.

[41] S. Rippa, Long and thin triangles can be good for linear interpolation, SIAM J. Numer. Anal. 29, 1, 257–270, 1992.

[42] K.G. Siebert. An a posteriori error estimator for anisotropic refinement. Numerische Mathematik, 73:373–398, 1996.

[43] R.B. Simpson, Anisotropic mesh transformations and optimal error control, Appl. Numer. Math., 14, 183–198 1994.

[44] M. Shephard Approaches to the automatic generation and control of finite element meshes, Appl. Mech. Rev. 41,4, 169-185, 1998.

[45] M. Shephard, Private communication, 1998.

[46] G. Strang and G.J Fix . An Analysis of the Finite Element Method. Prentice Hall Series in Automatic Computation, Englewood Cliffs N.J., 1973.

[47] W.C. Thacker, A brief review of techniques for generating irregular computational grids. Int. Jour. for Num. Meths. in Engng. 15, 1980, 1335-1341.

[48] N.P. Weatherill, M.J. Marchant and O.Hassan, Unstructured grid generation and adaptation for a transport aircraft configuration. Paper presented at 1993 European Forum on Recent Developments and Applications in Aeronautical Computational Fluid Dynamics. Held at Bristol UK 1-3 September 1993.

[49] M. Zlamal On the Finite Element Method. Numer. Math. v.12, 394-409, 1968.